Journal of Biomechanics 46 (2013) 2477–2482

Contents lists available at ScienceDirect

Journal of Biomechanics

journal homepage: www.elsevier.com/locate/jbiomech
www.JBiomech.com

Filling the void: A coalescent numerical and experimental technique to determine aortic stent graft mechanics

S. De Bock [a,*], F. Iannaccone [a], M. De Beule [a,b], D. Van Loo [c], F. Vermassen [d], B. Verhegghe [a,b], P. Segers [a]

[a] IBiTech-bioMMeda, Ghent University, De Pintelaan 185-Block B, BE-9000 Ghent, Belgium
[b] FEops bvba, Ghent, Belgium
[c] Centre for X-ray Tomography (UGCT), Ghent University, Belgium
[d] Department of Thoracic and Vascular Surgery, Ghent University Hospital, Ghent, Belgium

ARTICLE INFO

Article history:
Accepted 9 July 2013

Keywords:
Abdominal aortic aneurysm
Stent graft
Finite element
Radial force

ABSTRACT

The presented study details a combined experimental and computational method to assess and compare the mechanical behavior of the main body of 4 different stent graft designs. The mechanical response to a flat plate compression and radial crimping of the devices is derived and related to geometrical and material features of different stent designs. The finite element modeling procedure is used to complement the experimental results and conduct a solution sensitivity study. Finite element evaluations of the mechanical behavior match well with experimental findings and are used as a quantitative basis to discuss design characteristics of the different devices.

1. Introduction

Abdominal aortic aneurysms (AAA) are dilatations of the aorta between the renal arteries and the aortic bifurcation. This weakened bulge can continue to expand, increasing the risk of rupture, a life-threatening scenario. The pathology can be repaired through open surgery or, less invasively, by endovascular aneurysm repair (EVAR) with a stent graft (SG). The endograft deployment technique and SG devices have advanced greatly in the last decade, yet they are still associated with long term problems, including graft migration or endoleakage (Schlosser et al., 2009; De Bruin et al., 2010) and material failings (Jacobs et al., 2003; Zarins et al., 2004).

A large number of competing SG devices have been approved for use in Europe. This offers different treatment opportunities for vascular surgeons and patients, yet, it also brings a challenge, as choosing and differentiating between devices is not always straightforward. In general, published comparisons between stent graft outcome are sparse (Wales et al., 2008; Mensel et al., 2012) and difficult to relate to actual patient morphology.

A factor that generally lacks in device comparisons are differences in stent graft designs related to the overall mechanical behavior of the device, leading to differing biomechanical forces at the implantation site. Stent grafts need to be oversized to have enough radial force to enforce adequate graft-wall contact (van Prehn et al., 2009). Amblard et al. (2009) confirmed, using finite element analysis, that a decrease in radial force can induce type I endoleak, and that oversize could help prevent endoleakage. On the other hand, increased radial force could have adverse effects on the aortic neck such as wall degeneration and neck dilation (van Prehn et al., 2009). Recently, Sincos et al. (in press) demonstrated in a porcine model that larger oversizing of thoracic stent grafts can lead to increased injury to the aortic wall.

A report on the mechanical properties of stent graft devices can: (1) assist in the design of new devices; (2) support the processing and interpretation of clinical trial data, e.g. when relating neck dilatation to the specific radial force of each stent design and oversize; and (3) move forward numerical studies on stent fatigue Kleinstreuer et al., 2008, or fluid structure interaction (Amblard et al., 2009; Prasad et al., 2012) to devices used in clinical practice. To our knowledge, there are no studies published investigating mechanical properties of clinically approved bifurcated aortic stent grafts.

In the present work, we use experimental and computational methods to assess and compare the behavior of the main body of 4 different SG designs: three nitinol based devices: Talent (Medtronic, Santa Rosa, Calif), Excluder (W.L.Gore and Associates, Flagstaff, Ariz) and Zenith LP (Cook Bloomington, Ind) and one stainless steel device: Zenith Flex (Cook Bloomington, Ind). Experimental set-ups are used to derive the mechanical response to a flat plate compression and radial crimping of the devices. Results from a computational modeling study are compared with the experiments to: (1) obtain the stent graft material properties via reverse

* Corresponding author. Tel.: +32 9 332 43 20; fax: +32 9 332 41 59.
E-mail address: Sander.DeBock@Ugent.be (S. De Bock).

0021-9290/$ - see front matter © 2013 Elsevier Ltd. All rights reserved.
http://dx.doi.org/10.1016/j.jbiomech.2013.07.010

engineering; (2) extend the loading range of the experimental radial crimp set-up and (3) extract the radial force for each individual segment. The use of 2 different experimental tests serves as a limited validation of the numerical method.

2. Material and methods

2.1. Stent graft devices

Stent grafts in general feature a membrane of polymer material that is supported by a metal frame or stent. They are crimped into a delivery device, inserted via the femoral artery and then advanced into position in the aortic aneurysm, where they are deployed.

The SG devices investigated in this study differ greatly in design and materials used. All devices are self-expanding. The devices differ in method and location of fixation. Suprarenal fixation is achieved by bare (uncovered) stent rings. Active fixation is achieved by outward pointing hooks at the proximal side of the devices while passive fixation relies on radial outward force and friction for proximal fixation. Table 1 lists the characteristics of the different devices included in the study. The listed diameters are the diameters of the investigated samples. Devices were visually inspected and measured using a caliper. High resolution microCT scanning was performed to get the 3D geometry of all devices (Mortier et al., 2008; De Bock et al., 2012).

2.2. Mechanical testing

The 4 devices were first subjected to a flat plate compression test. Tests were performed at body temperature (37 °C) using an Instron 5944 electromechanical test system (Instron, Norwood, MA, USA) with a *BioBox* temperature controlled air chamber.. The system was equipped with a 50 N load cell and two flat compression plates. The devices were compressed from their original diameter to 9 mm clearance between the plates. The complete main body of the device was tested.

The stent graft sections proximal to the bifurcation of all devices were subsequently subjected to a radial compression test, at body temperature. For this, a radial crimping head (MPT Europe, Leek, The Netherlands) was mounted on the electromechanical test system. The radial crimping head features an 8-segment iris to reduce the diameter of the inserted stent. The crimping head was limited to a maximum diameter of 22 mm. In this study, we were limited to one sample of each device. As they are self-expandable, one device can, however, be repeatedly mechanically tested without any permanent deformations. The devices were manually inserted into the crimping head and compressed to a diameter of 8 mm (nitinol devices) or 9 mm (stainless steel device) to avoid permanent deformations and material damage.

The first 2 segments of each device were inserted into the crimping head, as shown in Fig. 1. For the Excluder device, which consists of a continuous wire, the first 38 mm were inserted, until the start of the bifurcation. Unless specified differently, in all further use, diameters reported are those of the inscribed circle of the 8-segment iris.

2.3. Computational modeling

Finite element (FE) models of the metallic stents were reverse engineered from μCT scans. The wires were modeled using circular, linear Timoshenko beam sections. A comparison with solid elements was performed for a single segment, showing element type insensitivity for radial force, confirming previous results by Hall and Kasper (2006). The laser cut proximal stents of the Zenith LP device were modeled using rectangular beam sections. The graft covering the stent was added to the FE models by spline fitting circumferences of subsequent stent rings. The fabric was discretized with general purpose finite membrane strain triangular shell elements, using Simpson's rule for the shell section integration. In this study, shell thickness is reduced to have negligible bending stiffness. The choice for shell over (computationally more efficient) membrane elements was done to have a better contact behavior: membrane elements exhibit sharp folds between elements when compressed, causing difficulties in solving this already challenging contact problem. The covering membrane was connected to the stent frames using discrete, rigid connections.

The stainless steel was assumed linear elastic, with an estimated elastic modulus of 193 GPa and Poisson ratio of 0.25. This is consistent with wires used in medical devices of stainless steel alloys 302, 304LV or 316LVM (Fort Wayne Metals, 2013).

The exact material properties of the nitinol devices are unknown. The superelastic behavior of nitinol was modeled using a material subroutine, available in Abaqus, based on the model described by Auricchio and Taylor (1997). In an isothermic environment, assuming a Poisson ratio of 0.3, it has 8 parameters that describe its material response (see Rebelo et al., 2001, Auricchio and Taylor, 1997 and Appendix B). Fabric materials were modeled using a linear elastic material, with assumed Poisson ratio of 0.3. Flat plate and radial crimp head were considered rigid. The FE calculations were performed using Abaqus/Explicit 6.12 (SIMULIA, Dassault Systèmes), in a quasi-static dynamic analysis with negligible kinetic energy (less than 5% of internal energy).

Compressing plates (flat and radial) were modeled as rigid surface elements, and moved in displacement control. Boundary conditions on the devices were: contact with these rigid plates, contact between stent struts and membrane, and self-contact between different stent struts and membrane elements. All contact was enforced using the penalty contact algorithm with finite sliding.

For the flat plate numerical simulation, one node of the device was fixed in the y and z direction (x being direction of compression), while for the radial crimp simulation, one node of the device was fixed in the z direction (xy being the crimping plane). This was done to avoid rigid body movement.

Compression force output (to be related with experimental output) were the discrete contact forces, integrated over the nodes of the compressing plate(s). The radial force exerted by each segment was calculated by summing only the force vectors at the location of that segment. For the continuous Excluder device, the radial force of the first 20 mm was separated for an easier comparison with the other devices.

In the flat plate compression simulation, the complete stent graft is modeled. In the radial crimp test, the unstressed parts are left out for computational efficiency. The stent segment adjacent to those being crimped is still included (see Fig. 2). For the Excluder device, the next 30 mm is included.

To assess the sensitivity of the simulations to the assumed dimensions, design parameters and finite element parameters, we first performed a sensitivity study to assess how the variability of these parameters and modeling assumptions influences mechanical response (see Appendix B). The sensitivity study also ensured insensitivity of mesh density on the resulting forces.

Next, we used the results and experience obtained by this sensitivity study to estimate the material parameters of the actual devices (model calibration). Material properties were manually adjusted until finite element experiments reproduced both the experimental force-clearance (flat plate testing) and force-diameter (radial force testing) relationships. For the stainless steel stent graft, only the fabric parameters required calibration; all other stent grafts required calibration of both the nitinol and fabric model parameters. The procedure is described in detail in Appendix B. Simulation results for the stainless steel Zenith Flex device serve to

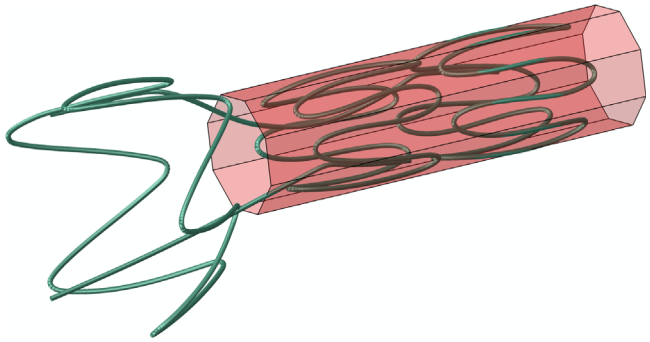

Fig. 1. Example crimping of first two stent rings. Finite element rendering for the Talent device, fabric not shown.

Table 1
Stent graft characteristics: stent material, graft material, fixation method, outer diameter, delivery system diameter and FDA status (March 2013) (1 Fr.=1/3 mm).

	Stent material	Graft material	Fixation	Diameter	Delivery diameter	FDA approved
Talent	Nitinol	Woven polyester	Passive suprarenal	28 mm	22 Fr.	Yes
Excluder	Nitinol	Expanded PTFE	Active infrarenal	26 mm	18 Fr.	Yes
Zenith Flex	Stainless steel	Woven polyester	Active suprarenal	30 mm	20 Fr.	Yes
Zenith LP	Nitinol	Woven polyester	Active suprarenal	30 mm	18 Fr.	Investigational use